Published Ahead of Print on September 16, 2020 as 10.1212/WNL.0000000000010868

OPEN

Neurology®

The most widely read and highly cited peer-reviewed neurology journal
The Official Journal of the American Academy of Neurology

AMERICAN ACADEMY OF NEUROLOGY®

Neurology Publish Ahead of Print
DOI: 10.1212/WNL.0000000000010868

Contribution of iron and Aβ to age differences in entorhinal and hippocampal subfield volume

Chris M. Foster, PhD; Kristen M. Kennedy, PhD; Ana M. Daugherty, PhD; Karen M. Rodrigue, PhD

The Article Processing Charge was funded by Dr. Karen Rodrigue.

Chris Foster, The University of Texas at Dallas, School of Behavioral and Brain Sciences, Center for Vital Longevity, Dallas, TX USA

Kristen Kennedy, The University of Texas at Dallas, School of Behavioral and Brain Sciences, Center for Vital Longevity, Dallas, TX USA

Ana Daugherty, Wayne State University, Department of Psychology, Department of Psychiatry and Behavioral Neurosciences, Institute of Gerontology, Detroit, MI

Karen Rodrigue, The University of Texas at Dallas, School of Behavioral and Brain Sciences, Center for Vital Longevity, Dallas, TX USA

Search Terms: 26 Alzheimer's disease, 36 Cognitive aging, 120 MRI, 122 PET, 130 Volumetric MRI

Submission Type: Article
Title Character count: 92
Number of Tables: 3
Number of Figures: 3
Word count of Abstract: 250
Word Count of Paper: 4163

Corresponding Author: Karen M. Rodrigue, krodrigue@utdallas.edu

Study Funding: Avid Radiopharmaceuticals/Eli Lilly, NIH (AG036848, AG036818, AG057537), Alzheimer's Association NIRG-397220, BvB, and AWARE.

This study was sponsored in part by Investigator Initiated Trial grant from Eli Lilly and Company for the Amyvid ligand, support from BvB Dallas and AWARE, as well as grants NIH (AG036848, AG036818, AG057537), and Alzheimer's Association NIRG-397220.

Disclosures: The authors report no disclosures relevant to the manuscript.

Statistical Analysis conducted by Dr. Chris M. Foster, The University of Texas at Dallas, School of Behavioral and Brain Sciences, Center for Vital Longevity, Dallas, TX USA

Abstract:

Objective: To test the hypothesis that the combination of both elevated global Aβ burden and greater striatal iron content would be associated with smaller entorhinal cortex (ERC) volume, but not hippocampal subfield volumes, we measured volume and iron content using high resolution MRI and Aβ using PET imaging in a cross-sectional sample of 70 cognitively normal older adults.

Methods: Participants were scanned using Florbetapir 18F PET to obtain amyloid-beta standardized uptake value ratios. Susceptibility-weighted MRI was collected and processed to yield R2* images and striatal regions-of-interest (ROIs) were manually placed to obtain a measure of striatal iron burden. Ultra-high-resolution T2/PD weighted MR images were segmented to measure MTL volumes. Analyses were conducted using mixed-effects models with MTL ROI as a within-subject factor and age, iron content, and Aβ as between-subjects factors and MTL volumes (ERC and three hippocampal subfield regions) as the dependent variable.

Results: The model indicated a significant four-way interaction among age, iron, Aβ, and MTL region. Post-hoc analyses indicated the three-way interaction among age, Aβ, and iron content was selective to the ERC (β = -3.34, *SE* = 1.33, 95%CI[-5.95, -0.72]), where a significant negative association between age and ERC volume was only present in individuals with both elevated iron content and Aβ.

Conclusions: These findings highlight the importance of studying Aβ in the context of other, potentially synergistic age-related brain factors, such as iron accumulation, as well as highlighting the potential role for iron as an important contributor to the earliest, preclinical stages of pathological aging.

1 Introduction

Aβ accumulation may be the earliest *in vivo* biomarker of AD[1,2], yet, the deleterious effects of Aβ on the brain have been difficult to establish[3]. A prevalent hypothesis suggests that excessive Aβ promotes oxidative stress[3,4]. Brain iron accumulation is a proxy indicator of oxidative stress that may shed some light on the effect of Aβ on the brain. In the course of aging, non-heme iron accumulates outside of binding complexes and promotes oxidative stress[5–8]. A disruption of iron homeostasis is also thought to play a significant role in the conversion of normal Aβ monomers into toxic Aβ oligomers and plaques[5,9], and some evidence suggests non-heme iron exacerbates the toxicity of Aβ to a variety of cellular membranes[10].

The entorhinal cortex (ERC) is a target of early AD-related pathology[11,12] and may exhibit structural changes associated with oxidative stress early in the disease cascade. Notably, as compared to volumes of the hippocampus and its subfields, ERC volumes in nonpathological aging are relatively stable across the adult lifespan[13,14]. Volumetric differences in the ERC may therefore be indicative of accelerated cognitive aging[15] or represent underlying AD-related changes[12,16].

The current study aimed to assess associations among early markers of AD, Aβ and brain iron content, on ERC and hippocampal subfield volumes in cognitively normal older adults. We hypothesized that 1) striatal brain iron content would be positively associated with Aβ burden and 2) elevated Aβ burden and striatal iron content would be related to smaller ERC volume in older adults, but not hippocampal subfield volumes.

2 Methods

2.1 Participants

Seventy participants (Age: *M* = 68.29, *SD* = 10.48, range 51 – 94) with complete PET and MR imaging data were drawn from a larger sample of individuals recruited from the Dallas-Fort Worth metroplex and with data collection occurring between 2013 and 2016. All participants in the current analysis underwent cognitive testing consisting primarily of standardized neuropsychological instruments, as well as MRI and PET scanning. Participants were all right-handed, native English speakers, screened to be free from a history of neurologic, cardiovascular, psychiatric, or metabolic disorders, substance abuse, or head injuries with a loss of consciousness greater than five minutes, and were required to score ≥ 26 on the Mini-Mental State Exam (MMSE)[17], and score less than or equal to 16 on the Center for Epidemiological Study – Depression (CESD)[18]. Participants were required to be 50 years of age or older to participate in PET imaging. Thirty-six eligible participants from the larger sample did not complete PET imaging. Those individuals were not significantly different on any demographic variable – age (*M* = 66.42, 95%CI[62.95, 69.88]), CESD (*M* = 4.81, 95%CI[3.48, 6.13]), education (*M* = 15.22, 95%CI[14.29, 16.16]), MMSE (*M* = 28.67, 95%CI[28.38, 28.96]) – from the seventy included in the current analysis. See Table 1 for sample demographic information.

2.2 Neuroimaging Protocol

2.2.1 MRI Acquisition

MR images were collected at the University of Texas Southwestern Medical Center's Advanced Imaging Research Center on a single 3T Philips Achieva whole-body scanner (Phillips Medical Systems, Andover, Massachusetts) equipped with a 32-channel head coil. Regional iron content was assessed using a T2* weighted multi-echo 3D gradient-recalled echo (GRE) sequence (65

axial slices, eight echo times: 5.68 ms +Δ 2.57 ms, FA = 15°, TR = 37 ms, FOV = 256 mm^2, 512 x 512 x 65 matrix, voxel size = 0.5 x 0.5 x 2 mm^3, 10:14 min). Regional medial temporal lobe (MTL) volumes were assessed from an ultra-high resolution T2/PD weighted image of the MTL aligned along the longitudinal axis of the hippocampus (TR = 3500 ms, TE = 44 ms, FOV = 215 x 215 mm, voxel size = .42 x .42 x 2.00 mm^3, 30 coronal slices, FA = 120°, total time = 6:46) and facilitated by collection of a T1-weighted high resolution MP-RAGE sequence (TR = 8.3ms, TE = 3.8ms, FOV = 256 x 204 mm, voxel size = 1 x 1 x 1 mm^3, 160 sagittal slices, FA = 12°, total time = 3:57 min).

2.2.2 Iron Content Processing

The T2* weighted GRE images were processed to produce R2* images according to a pipeline utilized in our prior reports[19,20]. Images were processed and masked in the Signal Processing in NMR software package (SPIN; MR Innovations, Inc., Detroit, MI, USA: http://mrinnovations.com/spin-lite; last accessed 03/29/2019). R2*, for which higher intensity values indicate relatively greater iron concentration, was calculated as the inverse of T2* at each voxel. Circular masks (24-pixels each) were manually placed within the bilateral caudate nucleus and putamen to estimate iron content (see Figure 1). Four masks were placed on a single image slice within each region per hemisphere and this was continued for 3 contiguous slices (see [21] for detailed procedure). Masks were placed by a single individual C.M. who was trained by A.M.D. Reliability was assessed with ICC(2) using a sample of 10 participants [22]. In the reported analyses, iron estimates were averaged across the regions of interest to calculate a single estimate of striatal iron content. The striatum accumulates iron across the lifespan and is sensitive to disruption of whole-brain iron homeostasis[23,24], therefore the measurement was used here as an indicator of general age-related risk for oxidative stress in the brain.

----------Figure 1 about here----------

2.2.3 Medial Temporal Lobe Volumes

Volumes for the four MTL regions-of-interest (ROI), including the ERC, subiculum, cornu-ammonis 1-2 (CA1/2), and cornu-ammonis 3/dentate gyrus (CA3/DG), were estimated using a semi-automated pipeline (see [25] for detailed procedure). Manual tracings of MTL ROIs were completed for 30 participants across the lifespan of the entire sample using recommendations from the hippocampal subfield harmonization workgroup[26]. The Automatic Segmentation of Hippocampal Subfields (ASHS) v1.0.0 software was then used to create a study specific atlas and apply machine-learning algorithms to segment all subfields for all the participants[27]. All MTL ROI volumes were summed across hemispheres and adjusted for intracranial volume using the analysis of covariance approach[28].

2.2.4 PET Acquisition

Positron emission tomography (PET) scans were collected on a Siemens ECAT HR PET scanner housed at UT Southwestern Medical School. Participants were injected with 370 MBq (10 mCi) of ^{18}F-Florbetapir (Avid Radiopharmaceuticals/Eli Lilly). Approximately 30 minutes post-injection, participants were placed on the imaging table. A 2-minute scout was acquired to ensure the brain was within the field of view. Fifty minutes post-injection, an internal rod source transmission scan was acquired for 7 minutes immediately followed by a 2-frame by 5 minutes each dynamic emission acquisition. The transmission image was reconstructed using back-projection with a 6-mm full-width at half-maximum (FWHM) Gaussian filter. Emission images were processed by iterative reconstruction, 4 iterations and 16 subsets with a 3-mm FWHM ramp filter.

2.2.5 PET Processing

Each participant's PET scan was first registered to their T1-weighted image with a rigid registration followed by an affine registration using Advanced Normalization Tools (ANTs)[29] scripts and visually inspected for registration quality. Freesurfer v5.3[30] parcellations of interest that correspond to the traditionally used 7 ROIs for amyloid deposition (i.e., anterior cingulate, posterior cingulate, precuneus, lateral temporal, lateral parietal, middle frontal, and inferior frontal) were also registered to each subject's T1 image. Using methods outlined in [31], uptake counts were extracted from each ROI, normalized to whole cerebellar counts to yield standardized uptake value ratios (SUVRs) for each ROI, and averaged to form a mean cortical amyloid index.

2.3 Genetic Protocol

A full description of the genetic protocol can be found in[32]. In brief, saliva collection was conducted using Oragene kits. Genetic analysis was performed at the University of Texas Southwestern Medical Center Microarray Core Facility. APOE status (rs429358 and rs7412) was acquired using TaqMan SNP Genotyping assays (Applied Biosystems).

2.4 Data Analysis Approach

To test our first hypothesis, that striatal non-heme iron content and global Aβ burden would exhibit a positive association, we conducted a bivariate correlation. To assess the potential influence of age on this association we ran the same correlation controlling for age. We also conducted several bivariate associations derived from the regional Aβ SUVRs (medial frontal cortex, lateral temporal, lateral parietal, precuneus, and anterior and posterior cingulate) and iron content, as well as striatal SUVR (combined caudate and putamen) and iron content, to provide additional information about the potential associations between Aβ and iron concentration.

To test our second hypothesis, that ERC volume, as compared to three hippocampal subfield ROIs (subiculum, CA1/2 and CA3/DG), would be negatively associated with age, Aβ, and iron burden, we conducted a linear mixed effects model implemented in R v3.5.3 (R Core Team, 2019, downloaded March 11, 2019) using the *LmerTest*[34] package and Satterthwaite's correction for degrees of freedom. Wald confidence intervals were calculated using the *confint* command within R. This model utilized mean-centered age, SUVR, and striatal iron content as between-subjects factors, MTL ROI as a within-subject factor, and MTL ROI volume (mean-centered within each region) as the dependent variable, with a random effect of subject. Mean-centering independent variables allows for proper estimation of lower-order effects, and because mean differences in volume were of no interest in the current analysis we mean-centered within each MTL ROI. A four-way interaction (i.e., age x iron x SUVR x MTL ROI) as well as all subordinate two- and three-way interactions were included. Interactions were probed using simple effects or simple slopes estimates.

Outliers, or data points exhibiting potentially high leverage on the results were assessed using three strategies. First, we implemented a conservative sensitivity analysis where the top 5% and bottom 5% of residuals were removed from the analysis and the results recomputed. Second, we winsorized MTL volume within each ROI to 3 standard deviations and recomputed the results. Third, we conducted a robust mixed effects model using *robustlmm*[35]. Custom code was used to calculate Wald confidence intervals for the robust model.

APOE genotype information was collected on most of the sample (n = 66). A secondary analysis was conducted covarying for the effects of dichotomous APOE e4 status on the grand mean and regional volume by including APOE as a dichotomous factor (i.e., e4- or e4+) along with its interaction with MTL ROI.

2.5 Standard Protocol Approvals, Registrations, and Patient Consents.

This study was approved by the University of Texas at Dallas and the University of Texas Southwestern Medical Center Institutional Review Boards. Written informed consent was obtained from all participants.

2.6 Data Availability

Data can be made available upon request.

3 Results

----------Table 1 about here----------

3.1 Association between Aβ and Iron Content.

The bivariate correlation between Aβ and striatal iron content was not significant, ($r(68) = .130$, $p = .283$) (See Figure 2). This result was unchanged when controlling for age, ($r(67) = -.039$, $p = .753$). To further explore potential associations between iron content and SUVR we conducted correlations between measures in the regions used to calculate global SUVR, as well as an additional striatal region SUVR. There were no significant associations between iron content and SUVR in the lateral temporal, ($r(68) = .227$, 95%CI[-0.01, 0.44]), prefrontal ($r(68) = .195$, 95%CI[-.04, 0.41]), lateral parietal ($r(68) = .119$, 95%CI[-0.12, 0.34]), anterior cingulate ($r(68) = .072$, 95%CI[-0.17, 0.30]), posterior cingulate ($r(68) = .089$, 95%CI[-0.14, 0.32]), or precuneus cortices ($r(68) = .066$, 95%CI[-0.17, 0.30]), or between striatal SUVR and iron content, ($r(68) = .055$, 95%CI[-0.18, 0.29]).

----------Table 2 about here----------

3.2 Effects of Aβ, Iron Content and Age on MTL ROIs.

The results of the linear mixed-effects model indicated one significant three-way interaction among SUVR, iron content, and MTL volume, ($F(3,186) = 3.85$, $p = .011$). We refrained from probing this interaction because it was qualified by the presence of a significant four-way

interaction among age, iron content, SUVR, and MTL volume, ($F(3,186) = 3.81$, $p = .011$). No other model *F*-tests were significant, *p*s > .141. Bivariate correlations among the predictor variables and MTL ROI volumes are presented in Table 2. Full model results for conditional effects are presented in Table 3.

We probed the four-way interaction by testing the three-way interaction (i.e., age x iron x SUVR) separately for each of the four MTL regions using the *glht* function from the *multcomp*[36] package and a false discovery rate (FDR) correction[37] for the seven post-hoc effect and difference estimates. A significant interaction among age, SUVR, and iron content was detected for the ERC (β = -3.34, $Z = -2.50$, $p\text{-}_{FDR} = .029$), whereas no other MTL regions exhibited this effect: Subiculum (β = 0.61, $Z = 0.46$, $p\text{-}_{FDR} = .711$), CA1/2 (β = -0.79, $Z = -0.59$, $p\text{-}_{FDR} = .711$), CA3/DG (β = 0.49, $Z = 0.37$, $p\text{-}_{FDR} = .711$). Further, the interaction among age, SUVR, and iron content detected in the ERC was significantly stronger than the same three-way interaction in all other hippocampal subfields: subiculum (β = 3.95, $Z = 2.97$, $p\text{-}_{FDR} = .013$), CA3/DG (β = 3.83, $Z = 2.88$, $p\text{-}_{FDR} = .014$), except CA1/2 (β = 2.55, $Z = 1.92$, $p\text{-}_{FDR} = .097$; see Table 3 for confidence intervals of differences).

To probe the three-way interaction effect on the ERC, we utilized a simple slopes analysis to assess the nature of the relationship between age and volume at varying levels of iron and amyloid loads. The results indicated a significant positive relationship between age and ERC volume that roughly corresponded to amyloid SUVR levels greater than 1.15 and iron content less than 30 $R2^*s^{-1}$ (see Figure 3). Additionally, a significant negative relationship between age and ERC volume was present at values of amyloid SUVR greater than 1.15 and iron values greater than roughly 45 $R2^*s^{-1}$ (see Figure 3).

3.3 Supporting Analyses.

To assess the potential influence of outliers on the results we conducted three follow-up analyses: a sensitivity analysis, winsorization of the volumetric data to 3 SD, and a robust mixed effects model. The sensitivity analysis revealed a similar, albeit non-significant effect, for the four-way interaction between age, SUVR, iron content, and MTL region, ($F(3,161.28) = 2.38$, $p = .072$) whereas the four-way interaction remained significant in the winsorized analysis, ($F(3,186) = 2.70$, $p = .047$). The interaction among age, SUVR, and iron content in the ERC was again similar but non-significant in the sensitivity analysis, (β = -1.96, SE = 1.21, 95%CI[-4.33, 0.42]), and the robust mixed effects model, (β = -2.19, SE = 1.24, 95%CI[-4.62, 0.24]), but remained significant in the winsorized analysis, (β = -2.65, SE = 1.32, 95%CI[-5.23, -0.07]). In each of these models, the age, SUVR, iron content interaction in the ERC was significantly stronger as compared to the subiculum – sensitivity analysis: (β = 2.49, SE = 1.05, 95%CI[0.43, 4.55]); winsorized analysis (β = 3.26, SE = 1.31, 95%CI[0.70, 5.82]); robust analysis: (β = 2.79, SE = 1.17, 95%CI[0.51, 5.08]) – and CA3/DG – sensitivity analysis: (β = 2.26, SE = 1.05, 95%CI[0.21, 4.30]); winsorized analysis: (β = 3.14, SE = 1.31, 95%CI[0.58, 5.71]); robust analysis: (β = 2.59, SE = 1.17, 95%CI[0.31, 4.87])), as was seen in the primary analysis. Finally, we investigated residual normality in both the fixed effect and random effect components. In the full model, there were significant, but small deviations from normality only in the fixed effect residuals as evidenced by a Shapiro-Wilk test ($W = .99$, $p = .022$). However, this is not the case in the sensitivity analysis ($W = .99$, $p = .269$), and the primary findings were retained. Taken together, the pattern of findings is largely stable across several approaches used to investigate subjects and data points with potentially high leverage on the results.

In order to test the potential influence of APOE, a secondary analysis covarying for APOE e4 status was conducted. A similar set of results to the primary analysis was found, such that there

was a significant three-way interaction among MTL ROI, SUVR, and iron content ($F(3,171) = 4.76$, $p = .003$), and a significant four-way interaction among MTL ROI, Age, SUVR, and iron content, ($F(3,171) = 4.24$, $p = .006$). No other effects were significant and there was no effect of APOE on the grand mean volume ($F(1,57) = 0.28$, $p = .596$) or regional MTL volume ($F(3,171) = 1.68$, $p = .174$). The three-way interaction among age, SUVR, and iron content in the ERC was significant (β = -1.99, SE = 0.68, 95%CI[-3.31, -0.67]), and in this case, greater as compared to the effect in the subiculum (β = 2.16, SE = 0.68, 95%CI[0.83, 3.49]), CA1/2 (β = 1.61, SE = 0.68, 95%CI[0.66, 3.31]), and CA3/DG (β = 1.99, SE = 0.68, 95%CI[0.28, 2.94]).

----------Figure 2 about here----------
----------Table 3 about here----------
----------Figure 3 about here----------

4 Discussion

The current *in vivo* study investigated the potential combined effect of global Aβ deposition and striatal iron concentration – proxy measures for AD pathology and oxidative stress – on age-related differences in hippocampal subfield and ERC volumes in a sample of cognitively normal adults. In line with our hypotheses, results indicated an interactive effect of Aβ, iron content and age on ERC volume specifically, where a negative association between age and ERC volume was only present in individuals with both elevated iron *and* elevated Aβ loads. Overall, the results suggest that iron concentration may work in synergy with Aβ to impact structural integrity of a key region of the medial temporal lobe, the ERC, which is altered early in the AD pathological cascade.

In individuals with elevated Aβ, age-related differences in ERC volume were dependent upon brain iron concentration. Age was positively correlated with ERC volume in individuals with relatively low iron concentration (R2* approximately 30 s^{-1}), whereas age was negatively correlated with ERC volume in individuals with relatively high iron concentration (R2* > 45 s^{-1}).

Consistent with the hypothesized synergistic effect, the association strengthened following a continuum as both Aβ and iron concentration increased. Based upon hypothesized models[24,38,39], smaller ERC volume in older age with these elevated biomarkers is likely driven by deleterious effects of oxidative stress and chronic inflammation on neurons, myelin, and other surrounding tissue. Further, Aβ oligomers form around a core of iron and these oligomers are associated with the production of hydrogen peroxide, which is pro-apoptotic and cytotoxic[5,9]. The bi-directional relation between Aβ and iron dys-homeostasis, further exacerbated by feedback loops involving oxidative stress and pro-inflammatory cytokines, accelerates the deleterious cycle that may lead to neuronal damage and eventually cell death, and the release of more iron from damaged, iron-rich oligodendrocytes[5,40]. Additionally, the anatomical cascade of AD begins in the perirhinal cortex (including ERC), and typically, after the onset of cognitive symptoms, moves into inferior temporal and hippocampal regions[11]. In our sample of cognitively-normal individuals, these associations were not only limited to the ERC, but significantly weaker and close to zero in the hippocampal subfield regions. The lack of independent effects of Aβ or iron content on any region also highlights that the interplay between these measures is critical to elucidating their impact on the brain.

A prior report from our group indexed lifespan age differences in iron concentration in the entorhinal cortex, and greater iron concentration partially explained smaller regional volumes among older adults, but not middle-aged and younger adults[41]. The current report is consistent with this observation and extends it further to account for elevated risk for AD indicated by high Aβ. The resource-intensive and iron-dependent myelination processes that mark protracted development of ERC late into the lifespan[40] may make the region particularly prone to oxidative stress, inflammation and amyloid deposition. Although both Aβ and iron concentration are

critical to normal cell function[24,40], it is the paradox of AD that excessive accumulation of either may initiate a neurodegenerative cascade. Indeed, the reported evidence is consistent with histological and animal studies that suggest Aβ acts synergistically with dysregulated iron and may result in Aβ oligomers and plaques, and oxidative stress[5,9,42].

It is important to note that the combined effects of Aβ and iron content on the association between age and ERC volume were limited to individuals with Aβ levels roughly above 1.15, a value above the recommended clinical cutoff for florbetapir positivity of 1.11[43]. Thus, in the range of iron values measured in the current study, iron in the absence of clinically-elevated Aβ was not associated with age-related volume differences in the ERC. It is likely that there are significant individual differences in susceptibility and response to oxidative stress. Individuals without significant Aβ burden, but who exhibit high levels of iron, may either be resilient to elevated levels of iron, or there may exist another mechanism that prevents iron from triggering the creation of Aβ.

The hypothesized effect was observed on a continuum that also included a positive association between age and ERC volume in individuals with elevated Aβ but low iron content, which was unexpected. Protracted development and maintenance of ERC is consistent with non-pathological aging[14,44]. Iron is necessary for neuronal function but its accumulation within age-sensitive regions is an antecedent to metabolic dysfunction, oxidative stress, chronic inflammation and cell death[7,8]. The consequences of iron accumulation are observed across the adult lifespan as neuronal dysfunction indicated by fMRI[45,46], regional brain shrinkage[20,47] and cognitive decline[19,20]. Therefore, non-heme iron homeostasis is of the utmost priority to maintain brain health and function. As Aβ binds soluble non-heme iron in the extracellular space[3,42], it is plausible that Aβ may help to prevent iron-related oxidative stress and promote maintenance of

ERC volume. Indeed, a previous study has reported positive associations between Aβ and MTL volume including the hippocampus and surrounding cortex[48], and approximately 20-30% of cognitively-normal individuals have significant Aβ burden[1,31]. Taken together, this suggests Aβ is not solely degenerative and its association with pathology may depend upon other biological factors, including iron concentration. In this manner, evidence of high iron concentration *and* high Aβ may indicate a distressed system that cannot sufficiently regulate and is at risk for AD-related pathology.

AD is thought to be associated with a physiological cascade where deleterious processes occur in a specific order. The current study provides evidence that in cognitively-normal adults, iron and Aβ exhibit a synergistic effect across older age on ERC volume; however, it will be critical for future research to investigate these processes longitudinally. Despite hypotheses of synergism between Aβ and iron accumulation across the lifespan, it is not clear on what time scales these antecedent processes may occur, or whether some individuals may be more or less resistant to oxidative stress and chronic inflammation. Although we hypothesized these effects would more likely appear in the ERC – namely due to its volumetric preservation in healthy aging and early sensitivity to AD pathology – as compared to the hippocampus, it is possible longitudinal studies would be better suited to separate the effects of AD pathology-associated volumetric decline from age-related change. The ERC is thought to be among the earliest sites of AD pathology, however, hippocampus is also known to be associated with AD pathology early in the disease[11]. Thus, the cross-sectional nature of the current study may contribute to the lack of synergistic effects of Aβ and iron content within the hippocampus. Additionally, the current study utilized reliable, well-validated approaches to measure both striatal iron and global Aβ across the cortex.

Future research will be needed to investigate potential local associations of iron and Aβ concentrations within the MTL regions in the context of AD pathology.

A key limitation in the current study was the lack of Tau measurements in our sample. While the literature suggests a specific role for iron in the accumulation of Aβ oligomers, iron is also thought to play a role in the formation of Tau[49] and there is evidence for an association between iron and Tau in clinical stages of AD[50]. Interestingly, in the current investigation, we find detrimental effects of age on ERC volume only in those with *both* elevated iron and Aβ, and not elevated Aβ alone. Because a significant portion of cognitively-normal adults will present with elevated levels of Aβ and exhibit Tau pathology, iron homeostasis may be a critical factor in elucidating processes that provide cognitive resiliency for some individuals despite Aβ and tau accumulation. Iron concentration may also shed light on why some individuals accumulate significant tau without Aβ burden. It will be important for future research to investigate iron in the context of Aβ, tau, and cognition to better understand the complex processes underlying neural degeneration. Additionally, while the current study investigated non-heme brain iron, other metals (e.g., copper and zinc) also play a role in oxidative stress, specifically in conjunction with Aβ[5,42]. Therefore, iron presents as just one target for future investigations aiming to understand the myriad factors associated with increased risk for AD.

Prevailing models of AD suggest that elevated Aβ is one of the earliest measurable AD biomarkers, followed by tau accumulation and MTL atrophy[2]. Each of these events in the cascade occurs before the onset of cognitive symptoms, highlighting the need to investigate factors associated with an increased risk for AD in cognitively normal samples. The present study finds that iron and Aβ act synergistically, indicating a negative association between age and MTL volume is present only in the ERC and in individuals with elevated levels of iron and

Aβ. These findings highlight the potential role for iron as an important contributor to the earliest, preclinical stages of pathological aging.

Acknowledgements

This study was funded, in part, by grants from the National Institutes of Health R00 AG-036848, R00 AG-036818, R01 AG-056535, R01 AG-057537, Alzheimer's Association NIRG-397220, and an Investigator Initiated Trial grant from Eli Lilly and Company for the Amyvid ligand as well as support from BvB Dallas and AWARE. We thank Marci Horn and David Hoagey for assistance with PET image processing.

Appendix 1: Authors

Name	Location	Contribution
Chris M. Foster, Ph.D.	The University of Texas at Dallas, School of Brain and Behavioral Sciences, Center for Vital Longevity, Dallas, TX USA	Processed T2/PD weighted images; drafted the manuscript for intellectual content; analyzed and interpreted the data.
Kristen M. Kennedy, Ph.D.	The University of Texas at Dallas, School of Brain and Behavioral Sciences, Center for Vital Longevity, Dallas, TX USA	Designed and conceptualized the study; revised the manuscript for intellectual content; interpreted the data.
Ana M. Daugherty, Ph.D.	Wayne State University, Department of Psychology, Department of Psychiatry and Behavioral Neurosciences, Institute of Gerontology, Detroit, MI	Processed the R2* images; revised the manuscript for intellectual content.
Karen M. Rodrigue, Ph.D.	The University of Texas at Dallas, School of Brain and Behavioral Sciences, Center for Vital Longevity, Dallas, TX USA	Designed and conceptualized the study; revised the manuscript for intellectual content; interpreted the data.

REFERENCES

1. Jansen WJ, Ossenkoppele R, Knol DL, et al. Prevalence of Cerebral Amyloid Pathology in Persons Without Dementia: A Meta-analysis. JAMA. 2015;313:1924–1938.
2. Jack CR, Knopman DS, Jagust WJ, et al. Tracking pathophysiological processes in Alzheimer's disease: An updated hypothetical model of dynamic biomarkers. Lancet Neurol. 2013;12:207–216.
3. Chen G, Xu T, Yan Y, et al. Amyloid beta: structure, biology and structure-based therapeutic development. Acta Pharmacol Sin. 2017;38:1205–1235.
4. Selkoe DJ, Hardy J. The amyloid hypothesis of Alzheimer's disease at 25 years. EMBO Mol Med. 2016;8:595–608.
5. Lynch T, Cherny RA, Bush AI. Oxidative processes in Alzheimer's disease: the role of Aβ-metal interactions. Exp Gerontol. 2000;35:445–451.
6. Morris G, Berk M, Carvalho AF, Maes M, Walker AJ, Puri BK. Why should neuroscientists worry about iron? The emerging role of ferroptosis in the pathophysiology of neuroprogressive diseases. Behav Brain Res. 2018;341:154–175.
7. Ward RJ, Zucca FA, Duyn JH, Crichton RR, Zecca L. The role of iron in brain ageing and neurodegenerative disorders. Lancet Neurol. 2014;13:1045–1060.
8. Zecca L, Youdim MBH, Riederer P, Connor JR, Crichton RR. Iron, brain ageing and neurodegenerative disorders. Nat Rev Neurosci. 2004;5:863–873.
9. Plascencia-Villa G, Ponce A, Collingwood JF, et al. High-resolution analytical imaging and electron holography of magnetite particles in amyloid cores of Alzheimer's disease. Sci Rep. 2016;6:24873.
10. Ayton S, Wang Y, Diouf I, et al. Brain iron is associated with accelerated cognitive

decline in people with Alzheimer pathology. Mol Psychiatry. Epub 2019 Feb 18.

11. Braak H, Braak E. Frequency of stages of Alzheimer-related lesions in different age categories. Neurobiol Aging. 1997;18:351–357.
12. Van Hoesen GW. The human parahippocampal region in Alzheimer's disease, dementia, and ageing. Parahippocampal Reg Organ Role Cogn Funct. Oxford University Press; 2002. p. 270–295.
13. Raz N, Rodrigue KM, Head D, Kennedy KM, Acker JD. Differential aging of the medial temporal lobe: a study of a five-year change. Neurology. 2004;62:433–438.
14. Hasan KM, Mwangi B, Cao B, et al. Entorhinal Cortex Thickness across the Human Lifespan. J Neuroimaging. 2016;26:278–282.
15. Rodrigue KM, Raz N. Shrinkage of the Entorhinal Cortex over Five Years Predicts Memory Performance in Healthy Adults. J Neurosci. 2004;24:956–963.
16. Killiany RJ, Hyman BT, Gomez-Isla T, et al. MRI measures of entorhinal cortex vs hippocampus in preclinical AD. Neurology. 2002;58:1188–1196.
17. Folstein MF, Folstein SE, McHugh PR. "Mini-mental state". A practical method for grading the cognitive state of patients for the clinician. J Psychiatr Res. 1975;12:189–198.
18. Radloff LS. A Self-Report Depression Scale for Research in the General Population. Appl Psychol Meas. 1977;1:385–401.
19. Daugherty AM, Hoagey DA, Kennedy KM, Rodrigue KM. Genetic predisposition for inflammation exacerbates effects of striatal iron content on cognitive switching ability in healthy aging. Neuroimage. 2019;185:471–478.
20. Rodrigue KM, Daugherty AM, Haacke EM, Raz N. The role of hippocampal iron concentration and hippocampal volume in age-related differences in memory. Cereb

Cortex. 2013;23:1533–1541.

21. Daugherty AM, Hoagey DA, Kennedy KM, Rodrigue KM. Genetic predisposition for inflammation exacerbates effects of striatal iron content on cognitive switching ability in healthy aging. Neuroimage. 2019;185:471–478.

22. Shrout PE, Fleiss JL. Intraclass correlations: Uses in assessing rater reliability. Psychol Bull. 1979;86:420–428.

23. Daugherty AM, Raz N. Appraising the Role of Iron in Brain Aging and Cognition: Promises and Limitations of MRI Methods. Neuropsychol Rev. 2015;25:272–287.

24. Raz N, Daugherty AM. Pathways to Brain Aging and Their Modifiers: Free-Radical-Induced Energetic and Neural Decline in Senescence (FRIENDS) Model - A Mini-Review. Gerontology. 2018;64:49–57.

25. Foster CM, Kennedy KM, Hoagey DA, Rodrigue KM. The role of hippocampal subfield volume and fornix microstructure in episodic memory across the lifespan. Hippocampus. 2019;29:1206–1223.

26. Wisse LEM, Daugherty AM, Olsen RK, et al. A harmonized segmentation protocol for hippocampal and parahippocampal subregions: Why do we need one and what are the key goals? Hippocampus. 2017;27:3–11.

27. Yushkevich PA, Pluta JB, Wang H, et al. Automated volumetry and regional thickness analysis of hippocampal subfields and medial temporal cortical structures in mild cognitive impairment. Hum Brain Mapp. 2015;36:258–287.

28. Raz N, Lindenberger U, Rodrigue KM, et al. Regional brain changes in aging healthy adults: General trends, individual differences and modifiers. Cereb Cortex. 2005;15:1676–1689.

29. Avants BB, Tustison NJ, Song G, Gee JC. ANTS: Advanced Open-Source Normalization Tools for Neuroanatomy. Penn Image Computing and Science Laboratory; 2009.

30. Fischl B. FreeSurfer. Neuroimage. 2012;62:774–781.

31. Rodrigue KM, Kennedy KM, Devous MD, et al. β-Amyloid burden in healthy aging: Regional distribution and cognitive consequences. Neurology. 2012;78:387–395.

32. Kennedy KM, Reese ED, Horn MM, et al. BDNF val66met polymorphism affects aging of multiple types of memory. Brain Res. 2015;1612:104–117.

33. R Core Team. R: A language and environment for statistical computing. Vienna, Austria; 2019.

34. Kuznetsova A, Brockhoff PB, Christensen RHB. lmerTest Package: Tests in Linear Mixed Effects Models. J Stat Softw. 2017;82.

35. Koller M. robustlmm : An R Package for Robust Estimation of Linear Mixed-Effects Models. J Stat Softw. 2016;75.

36. Hothorn T, Bretz F, Westfall P. Simultaneous Inference in General Parametric Models. Biometrical J. 2008;50:346–363.

37. Benjamini Y, Hochberg Y. Controlling the False Discovery Rate: A Practical and Powerful Approach to Multiple Testing. J R Stat Soc Ser B. 1995;57:289–300.

38. Bartzokis G. Alzheimer's disease as homeostatic responses to age-related myelin breakdown. Neurobiol Aging. 2011;32:1341–1371.

39. Liu J-L, Fan Y-G, Yang Z-S, Wang Z-Y, Guo C. Iron and Alzheimer's Disease: From Pathogenesis to Therapeutic Implications. Front Neurosci. 2018;12.

40. Bartzokis G. Age-related myelin breakdown: A developmental model of cognitive decline and Alzheimer's disease. Neurobiol Aging. 2004;25:5–18.

41. Rodrigue KM, Haacke EM, Raz N. Differential effects of age and history of hypertension on regional brain volumes and iron. Neuroimage. 2011;54:750–759.

42. Maynard CJ, Cappai R, Volitakis I, et al. Overexpression of Alzheimer's disease amyloid-β opposes the age-dependent elevations of brain copper and iron. J Biol Chem. 2002;277:44670–44676.

43. Clark CM, Schneider JA, Bedell BJ, et al. Use of Florbetapir-PET for Imaging β-Amyloid Pathology. JAMA. 2011;305:275–283.

44. Graterón L, Insausti AM, García-Bragado F, et al. Postnatal development of the human entorhinal cortex. Parahippocampal Reg Role Cogn Funct. Oxford University Press; 2002. p. 20–31.

45. Kalpouzos G, Garzón B, Sitnikov R, et al. Higher Striatal Iron Concentration is Linked to Frontostriatal Underactivation and Poorer Memory in Normal Aging. Cereb Cortex. 2017;27:3427–3436.

46. Salami A, Avelar-Pereira B, Garzón B, Sitnikov R, Kalpouzos G. Functional coherence of striatal resting-state networks is modulated by striatal iron content. Neuroimage. 2018;183:495–503.

47. Daugherty AM, Haacke EM, Raz N. Striatal Iron Content Predicts Its Shrinkage and Changes in Verbal Working Memory after Two Years in Healthy Adults. J Neurosci. 2015;35:6731–6743.

48. Chételat G, Villemagne VL, Pike KE, et al. Larger temporal volume in elderly with high versus low beta-amyloid deposition. Brain. 2010;133:3349–3358.

49. Masaldan S, Bush AI, Devos D, Rolland AS, Moreau C. Striking while the iron is hot: Iron metabolism and ferroptosis in neurodegeneration. Free Radic Biol Med. Elsevier

B.V.; 2019;133:221–233.

50. van Duijn S, Bulk M, van Duinen SG, et al. Cortical Iron Reflects Severity of Alzheimer's Disease. J Alzheimer's Dis. 2017;60:1533–1545.

Table 1. Demographics and Summary Statistics

Demographics	Mean (SD)	Min	Max
Age	68.29 (10.48)	51	94
Sex (%F)	60.00		
Education	15.59 (2.60)	12	20
CESD	3.84 (3.65)	0	16
MMSE	28.83 (0.76)	26	30
Volume (mm^3)			
ERC	517.78 (87.10)	324.93	858.72
Subiculum	549.01 (69.48)	396.90	693.61
CA1/2	310.05 (40.39)	179.93	404.31
CA3/DG	445.49 (64.36)	304.47	633.63
Aβ and Iron			
SUVR	1.11 (0.16)	0.93	1.66
R2* (s^{-1})	30.78 (6.72)	20.23	54.56

Note. CESD = Center for Epidemiological Studies Depression, MMSE = Mini Mental State Exam, ERC = Entorhinal Cortex, CA = Cornu Ammonis, DG = Dentate Gyrus, SUVR = Aβ standardized uptake value ratio.

Table 2. Bivariate Correlations among Variables of Interest

	ERC	Subiculum	CA1/2	CA3/DG
Age	-.143 [-.37, .10]	-.213 [-.43, .02]‡	-.042 [-.27, .19]	-.173 [-.39, .07]
SUVR	-.179 [-.40, .06]	-.112 [-.34, .13]	-.113 [-.34, .12]	-.206 [-.42, .03]‡
R2* (s^{-1})	-.091 [-.32, .15]	-.039 [-.27, .20]	-.032 [-.27, .21]	-.124 [-.35, .12]

Note: Values represent zero-order correlations followed by the 95% confidence interval. Each correlation has 68 degrees of freedom. No bivariate correlations are significant. SUVR= Aβ standardized uptake value ratio, ERC = entorhinal cortex, CA = Cornu Ammonis, DG = dentate gyrus, R2* (s^{-1}) = measure of striatal non-heme iron content, ‡ = $p < .10$.

Table 3. Linear Mixed Effects Model Results Predicting MTL Volumes.

Effect	Est.	SE	df	*t*	*p*	95% CI
Intercept (ERC)	-5.03	8.76	140.88	-0.57	0.567	[-22.2, 12.14]
Age (ERC)	0.38	0.89	140.88	0.43	0.667	[-1.36, 2.13]
SUVR (ERC)	-120.32	79.9	140.88	-1.51	0.134	[-276.91, 36.27]
R2* (ERC)	1.74	1.56	140.88	1.11	0.268	[-1.32, 4.79]
CA1/2	4.89	8.73	186	0.56	0.576	[-12.22, 22.01]
CA3/DG	3.25	8.73	186	0.37	0.711	[-13.87, 20.36]
Sub	2.13	8.73	186	0.24	0.807	[-14.98, 19.25]
Age x SUVR (ERC)	14.68	8.78	140.88	1.67	0.097	[-2.52, 31.88]
Age x R2* (ERC)	-0.32	0.16	140.88	-2	0.048	[-0.63, -0.01]
SUVR x R2* (ERC)	37.27	13.58	140.88	2.75	0.007	[10.66, 63.88]
Age x CA1/2	-0.37	0.89	186	-0.41	0.68	[-2.11, 1.37]
Age x CA3/DG	-0.58	0.89	186	-0.66	0.513	[-2.32, 1.16]
Age x Sub	-1.22	0.89	186	-1.37	0.171	[-2.96, 0.52]
SUVR x CA1/2	116.95	79.62	186	1.47	0.144	[-39.1, 273]
SUVR x CA3/DG	-16.53	79.62	186	-0.21	0.836	[-172.58, 139.53]
SUVR x Sub	3.67	79.62	186	0.05	0.963	[-152.39, 159.72]
R2* x CA1/2	-1.5	1.56	186	-0.97	0.336	[-4.55, 1.55]
R2* x CA3/DG	-2.26	1.56	186	-1.45	0.148	[-5.31, 0.79]
R2* x Sub	-1.45	1.56	186	-0.93	0.352	[-4.5, 1.6]
Age x SUVR x R2* (ERC)	-3.34	1.33	140.88	-2.5	0.013	[-5.95, -0.72]
Age x SUVR x CA1/2	-16.63	8.75	186	-1.9	0.059	[-33.77, 0.51]

Age x SUVR x CA3/DG	-4.11	8.75	186	-0.47	0.639	[-21.25, 13.03]
Age x SUVR x Sub	-1.49	8.75	186	-0.17	0.865	[-18.63, 15.65]
Age x R2* x CA1/2	0.32	0.16	186	2.02	0.045	[0.01, 0.63]
Age x R2* x CA3/DG	0.16	0.16	186	1.05	0.297	[-0.14, 0.47]
Age x R2* x Sub	0.14	0.16	186	0.87	0.385	[-0.17, 0.45]
SUVR x R2* x CA1/2	-27.97	13.53	186	-2.07	0.04	[-54.49, -1.45]
SUVR x R2* x CA3/DG	-40.99	13.53	186	-3.03	0.003	[-67.51, -14.47]
SUVR x R2* x Sub	-38.44	13.53	186	-2.84	0.005	[-64.96, -11.92]
Age x SUVR x R2* x CA1/2	2.55	1.33	186	1.92	0.057	[-0.06, 5.15]
Age x SUVR x R2* x CA3/DG	3.83	1.33	186	2.88	0.004	[1.23, 6.43]
Age x SUVR x R2* x Sub	3.95	1.33	186	2.97	0.003	[1.35, 6.55]

Note. All variables mean-centered. Medial temporal lobe (MTL) volumes (mean-centered within each region-of-interest) were the dependent variable. Wald 95% confidence intervals are presented for each estimated effect. The ERC is the reference region. A random effect for subject was included in the model. ERC = entorhinal cortex, CA = cornu ammonis, DG = dentate gyrus, Sub = subiculum, SUVR = Aβ standardized uptake value ratio, R2* = measure of striatal non-heme iron content.

Figure 1. *Representative images from all neuroimaging modalities.* Panel A depicts hippocampal subfields (red = CA3/DG, orange = CA1/2, yellow = Subiculum) and ERC (shown in blue) volumes derived from ASHS. Panel B shows Amyvid PET scan for a cognitively normal participant with extensive beta-amyloid burden. Panel C illustrates an R2* (s^{-1}) image with manual probe placement in the caudate (red) and putamen (orange).

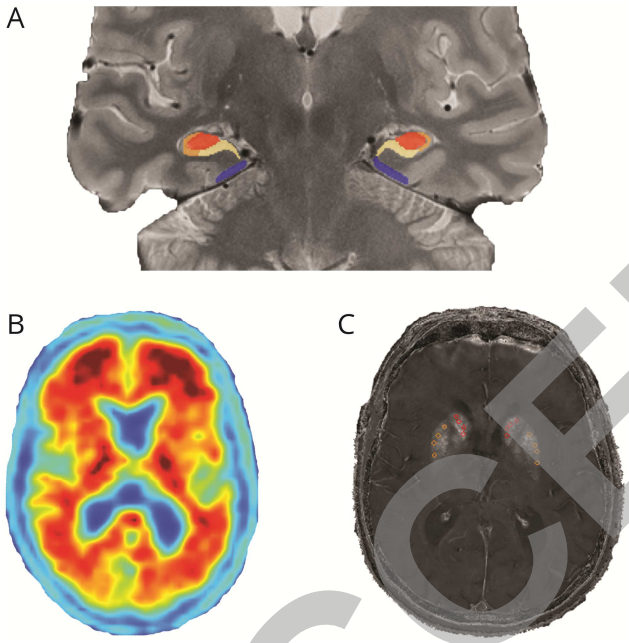

Figure 2. *Association between R2* and amyloid SUVR.* In the current sample of cognitively normal adults over the age of 50, there is no significant association between R2* (s^{-1}) (i.e., a measure of striatal iron content) and beta-amyloid burden.

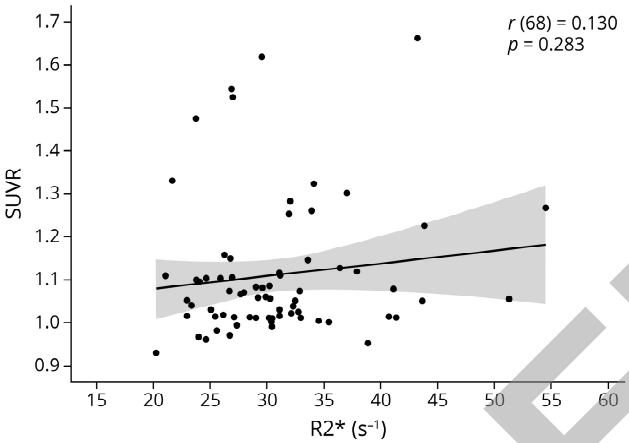

Figure 3. *Slope of age and ERC volume as a function of beta-amyloid SUVR and striatal iron.* The 4-way interaction is displayed as model implied simple slopes of age predicting entorhinal cortex (ERC) volume as a function of iron concentration (R2*) at three levels of beta-amyloid (Aβ) corresponding an SUVR of 1.1, 1.3, and 1.5, levels that correspond to increasing and clinically relevant levels of Aβ. At levels of Aβ SUVR below ~1.15 there is no independent relation between age and ERC volume, and no interaction with iron concentration. At levels of Aβ SUVR 1.15 and higher there is an association between age and ERC volume and the magnitude (and direction) of effect depends on iron concentration. For individuals with high iron concentration (roughly above 45s^{-1}) and high Aβ, there is a significant negative association between age and ERC volume (right side of light grey shading in panel 2 and 3) that strengthens as Aβ and iron increase. For individuals with low iron (roughly below 30s^{-1}) and high Aβ, there is a significant positive association between age and ERC volume (left side of light grey shading in panel 2 and 3) that strengthens with less iron and greater Aβ.

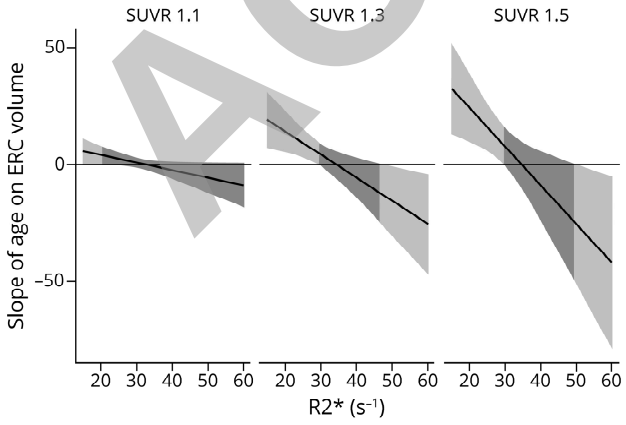

Contribution of iron and Aβ to age differences in entorhinal and hippocampal subfield volume

Chris M. Foster, Kristen M. Kennedy, Ana M. Daugherty, et al.

Neurology published online September 16, 2020
DOI 10.1212/WNL.0000000000010868